Published in final edited form as:
Bone. 2009 May ; 44(5): 1015–1017. doi:10.1016/j.bone.2009.01.376.

An Effective Histological Staining Process to Visualize Bone Interstitial Fluid Space Using Confocal Microscopy

Cesare Ciani, **Stephen B. Doty**[+], and **Susannah P. Fritton**[*]

Department of Biomedical Engineering, City College of New York, New York, NY 10031

[+] Research Division, Hospital for Special Surgery, New York, NY 10021

Abstract

Bone is a composite porous material with two functional levels of porosity: the vascular porosity that surrounds blood vessels and the lacunar-canalicular porosity that surrounds the osteocytes. Both the vascular porosity and lacunar-canalicular porosity are directly involved in interstitial fluid flow, thought to play an important role in bone's maintenance. Because of the small dimensions of the lacunar-canalicular porosity, interstitial fluid space has been difficult to visualize and quantify. We report a new staining protocol that is reliable and easily reproducible, using fluorescein isothiocyanate (FITC) as a probe visualized by confocal microscopy. Reconstructed FITC-stained cross sections enable effective visualization of bone microstructure and microporosities. This new staining process can be used to analyze interstitial fluid space, providing high-resolution quantification of the vascular pores and the lacunar-canalicular network of cortical and cancellous bone.

Keywords

microstructure; osteocyte; FITC; lacuna; canaliculi

Introduction

When bone is mechanically loaded, interstitial fluid flows through the small pores surrounding the osteocytes in the lacunar-canalicular porosity and drains into and out of the larger pores surrounding the blood vessels and nerves in the vascular porosity. This load-induced interstitial fluid displacement is thought to have two effects on bone: (a) enhancement of solute transport via convective mechanisms that affect maintenance of the tissue, and (b) activation of osteocytes via cytoskeletal deformations, thus playing a role in bone's mechanosensory system [1–6]. The annular interstitial fluid space bounded by the mineralized matrix and the osteocyte cell processes is of the order 100 nm [7], whereas the vascular pores are approximately 5–70 μm in diameter [8]; the water in the collagen-apatite porosity in the mineralized matrix is believed to be bound [9] and thus does not contribute to load-induced interstitial fluid flow. To better understand the processes of bone maintenance and adaptation it is important to accurately quantify cortical and cancellous bone microporosities, critical input parameters for models of interstitial fluid flow and mechanotransduction in bone.

*Corresponding author: Mailing address: Department of Biomedical Engineering, City College of New York, Convent Avenue at 138th Street, New York, NY 10031, 212-650-5213 (voice); 212-650-6727 (fax), fritton@ccny.cuny.edu.

Several groups have tried to visualize the interconnectedness of the vascular and lacunar-canalicular network and quantify bone porosities using different methods [10–14]. Unfortunately, the small size of the vascular and lacunar-canalicular pores, the low resolution of some of the imaging approaches used, and the restricted areas analyzed in some studies have been limitations of previous work. The decalcification of bone samples used in some previous studies might also induce histological artifacts [15]. To address these issues, we have developed an effective and easily reproducible technique to delineate and visualize bone interstitial fluid space using the fluorescent properties of fluorescein isothiocyanate (FITC), in conjunction with high resolution confocal microscopy.

Materials and Methods

For the protocol described rat bone was used (3-month-old male Sprague Dawley); however, the methods are not species-specific. To visualize cortical bone for this study, tibial cross sections were obtained from the mid-diaphysis as well as from the metaphysis approximately 2 mm distal to the growth plate. To visualize cancellous bone, longitudinal sections were obtained from the metaphysis and epiphysis of the proximal tibia.

Immediately after harvest, bones were placed in EM fixative (0.5% gluteraldehyde, 2% paraformaldehyde in 0.05M cacodylate-sodium buffer, pH 7.4) at room temperature and then immediately processed to obtain cortical sections and cancellous bone blocks. Cortical bone thick sections (300–400 μm) were cut with a diamond blade saw (Buehler, Lake Bluff, IL), the bone marrow washed out, and the sections placed back into EM fixative for 24 hours at room temperature. The cortical sections were then ground by hand to a final thickness of 30–50 μm using Carbimet paper discs (800 and 1200 grit; Buehler), and dehydrated in ascending graded ethanol (EtOH) (75%, 95%, and 100%, 5 minutes each). Cancellous blocks from the metaphyseal/epiphyseal region, approximately 10 mm × 10 mm × 10 mm, were placed into EM fixative for 48 hours at room temperature without bone marrow removal, and then dehydrated in ascending graded EtOH (75%, 95%, and 100%, 2 days each). To stain interstitial bone space we used FITC (fluorescein isothiocyanate isomer I from Sigma, product #F7250), diluted in 100% EtOH at a concentration of 1%. The solution was gently mixed in a rotator for approximately 1 hour at room temperature until clear, and then filtered. Cortical sections and cancellous blocks were then placed in 20 ml glass vials containing freshly prepared staining solution and gently mixed in a rotator for 4 hours at room temperature. The cortical sections were then rinsed in 100% EtOH for 30 minutes, air dried and coverslipped with mounting media (Richard-Allan Scientific, Kalamazoo, MI). The cancellous blocks were embedded in PMMA [16], then thick sections (400–500 μm) were cut and ground down to a final thickness of 40–70 μm using Carbimet paper discs (600 and 1200 grit; Buehler). Embedded cancellous sections were dried in ascending graded EtOH (75%, 95%, and 100%, 5 minutes each), air dried and coverslipped. During all the staining steps the sections, samples and vials were wrapped in aluminum foil to prevent loss of fluorescence.

All the sections were imaged using a confocal microscope (Leica TCS SP2, Germany) with the following parameters: 40× oil immersion lens, 1.25 numerical aperture, laser wavelength excitation of 488 nm, pinhole set at 1 Airy unit, 2048 × 2048 resolution giving a field of view of 375 × 375 μm, and laser intensity set at 12% of the full power. The gain and offset were chosen such that in the images acquired the canalicular system in both unembedded (cortical) and embedded (cancellous) sections covered the full dynamic range. A complete reconstruction of each cortical cross-section (tibia mid-diaphysis and metaphysis) was obtained using Photoshop 7.0 by overlaying adjacent bone section sectors imaged with the confocal microscope.

Results

Using the FITC staining protocol, unembedded cortical bone and PMMA-embedded cancellous bone sections showed the vascular and lacunar-canalicular porosities uniformly stained, with the mineralized matrix impermeable to the fluorescent probe (Figure 1). The high-resolution reconstructed sections (file size ~ 500 MB for the mid-diaphysis sections, and ~ 1.5 GB for the metaphysis sections) illuminated the microstructural details of the lacunar-canalicular network (Figure 2). The staining uniformity made it possible to distinguish detailed microstructural patterns such as regions with low canalicular density (Figure 2b, c).

Discussion

We have developed a consistent and effective histological method to stain interstitial fluid space using FITC as a fluorescent probe and confocal microscopy to visualize the bone microporosities. This staining technique also appears to be an effective method to obtain high-resolution images of an entire bone cross-section, helpful when visualizing the microstructural details of the lacunar-canalicular network. Although the reconstruction process used to obtain the images of the full cross-sections is somewhat tedious, a motorized stage connected to the confocal microscope would make the reconstruction process less time-consuming.

Compared to previously reported staining methods to delineate the lacunar-canalicular network and quantify bone porosity, the staining technique developed here presents several advantages: there is no need to decalcify the samples so the introduction of histological artifact is reduced; the staining technique is simple and fast, with a staining time of 4 hours for rat bone; and finally, it does not introduce areas that are either over- or under-stained. The technique can also be used to illuminate the porosity patterns of a whole bone section without being limited to a restricted region, an approach that was not utilized in previous studies. While this method is similar to the basic fuchsin method used to detect microdamage [17–19], we found that using FITC was more effective in staining the lacunar-canalicular pores with minimal background staining in the mineralized matrix.

The ability to visualize an entire cross-section makes this technique useful when analyzing and identifying bone macrostructure and bone microstructure, such as regions with either high or low canalicular density. The fluorescent properties of FITC and the high-resolution images could also be utilized to quantify the different microporosities in bone (vascular porosity and lacunar-canalicular porosity) and to obtain 3-D images to analyze bone permeability. Finally, this staining method can be easily adapted to different bone sizes, and different species.

Acknowledgments

This study was supported by a grant from the NIH (NIAMS, AR052866).

References

1. Han Y, Cowin SC, Schaffler MB, Weinbaum S. Mechanotransduction and strain amplification in osteocyte cell processes. Proc Natl Acad Sci U S A 2004;101:16689–94. [PubMed: 15539460]
2. Hillsley MV, Frangos JA. Bone tissue engineering: the role of interstitial fluid flow. Biotechnol Bioeng 1994;43:573–81. [PubMed: 11540959]
3. Klein-Nulend J, van der Plas A, Semeins CM, Ajubi NE, Frangos JA, Nijweide PJ, Burger EH. Sensitivity of osteocytes to biomechanical stress in vitro. Faseb J 1995;9:441–5. [PubMed: 7896017]
4. Piekarski K, Munro M. Transport mechanism operating between blood supply and osteocytes in long bones. Nature 1977;269:80–2. [PubMed: 895891]
5. Weinbaum S, Cowin SC, Zeng Y. A model for the excitation of osteocytes by mechanical loading-induced bone fluid shear stresses. J Biomech 1994;27:339–60. [PubMed: 8051194]

6. You L, Cowin SC, Schaffler MB, Weinbaum S. A model for strain amplification in the actin cytoskeleton of osteocytes due to fluid drag on pericellular matrix. J Biomech 2001;34:1375–86. [PubMed: 11672712]
7. You LD, Weinbaum S, Cowin SC, Schaffler MB. Ultrastructure of the osteocyte process and its pericellular matrix. Anat Rec A Discov Mol Cell Evol Biol 2004;278:505–13. [PubMed: 15164337]
8. Cooper RR, Milgram JW, Robinson RA. Morphology of the osteon. An electron microscopic study. J Bone Joint Surg Am 1966;48:1239–71. [PubMed: 5921783]
9. Nyman JS, Roy A, Shen X, Acuna RL, Tyler JH, Wang X. The influence of water removal on the strength and toughness of cortical bone. J Biomech 2006;39:931–8. [PubMed: 16488231]
10. Baylink DJ, Wergedal JE. Bone formation by osteocytes. Am J Physiol 1971;221:669–78. [PubMed: 5570322]
11. Kusuzaki K, Kageyama N, Shinjo H, Murata H, Takeshita H, Ashihara T, Hirasawa Y. A staining method for bone canaliculi. Acta Orthop Scand 1995;66:166–8. [PubMed: 7537935]
12. Li GP, Bronk JT, An KN, Kelly PJ. Permeability of cortical bone of canine tibiae. Microvasc Res 1987;34:302–10. [PubMed: 2448591]
13. Cooper DM, Matyas JR, Katzenberg MA, Hallgrimsson B. Comparison of microcomputed tomographic and microradiographic measurements of cortical bone porosity. Calcif Tissue Int 2004;74:437–47. [PubMed: 14961208]
14. Basillais A, Bensamoun S, Chappard C, Brunet-Imbault B, Lemineur G, Ilharreborde B, Ho Ba Tho MC, Benhamou CL. Three-dimensional characterization of cortical bone microstructure by microcomputed tomography: validation with ultrasonic and microscopic measurements. J Orthop Sci 2007;12:141–8. [PubMed: 17393269]
15. Ciani C, Doty SB, Fritton SP. Mapping bone interstitial fluid movement: displacement of ferritin tracer during histological processing. Bone 2005;37:379–87. [PubMed: 15964255]
16. Erben RG. Embedding of bone samples in methylmethacrylate: an improved method suitable for bone histomorphometry, histochemistry, and immunohistochemistry. J Histochem Cytochem 1997;45:307–13. [PubMed: 9016319]
17. Bentolila V, Boyce TM, Fyhrie DP, Drumb R, Skerry TM, Schaffler MB. Intracortical remodeling in adult rat long bones after fatigue loading. Bone 1998;23:275–81. [PubMed: 9737350]
18. Burr DB, Hooser M. Alterations to the en bloc basic fuchsin staining protocol for the demonstration of microdamage produced in vivo. Bone 1995;17:431–3. [PubMed: 8573418]
19. Burr DB, Stafford T. Validity of the bulk-staining technique to separate artifactual from in vivo bone microdamage. Clin Orthop Relat Res 1990:305–8. [PubMed: 1699696]

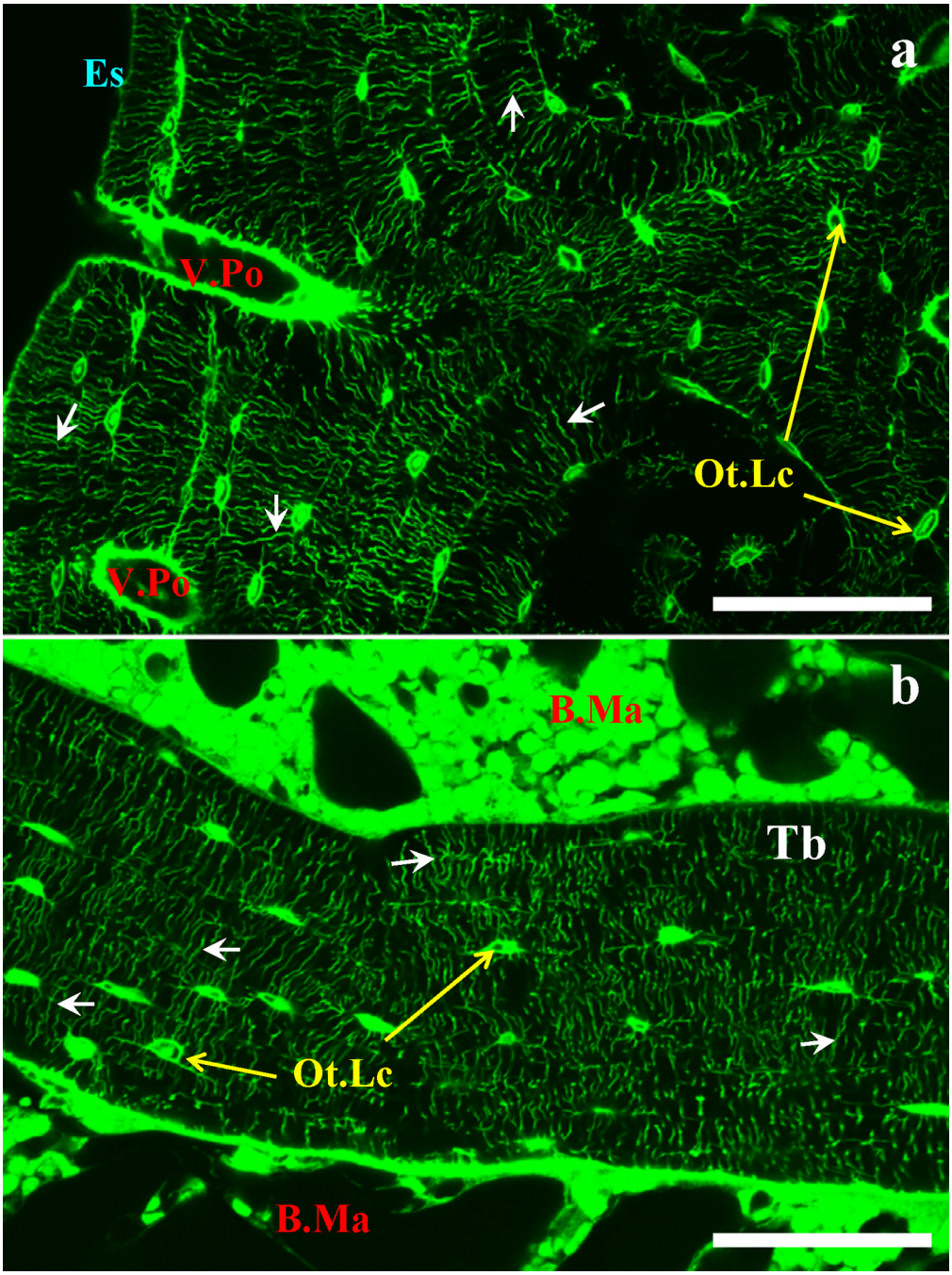

Figure 1.
(a) Unembedded cortical rat tibia diaphysis and (b) PMMA-embedded cancellous rat tibia metaphysis stained with FITC. The staining method demarcates the vascular porosity (V.Po), the canalicular porosity (small arrows), and the interstitial space surrounding the osteocyte lacunae (Ot.Lc) of both cortical and cancellous bone. Endosteal surface (Es), bone marrow (B.Ma), and trabecula (Tb) are also indicated; scale bars 130 μm.

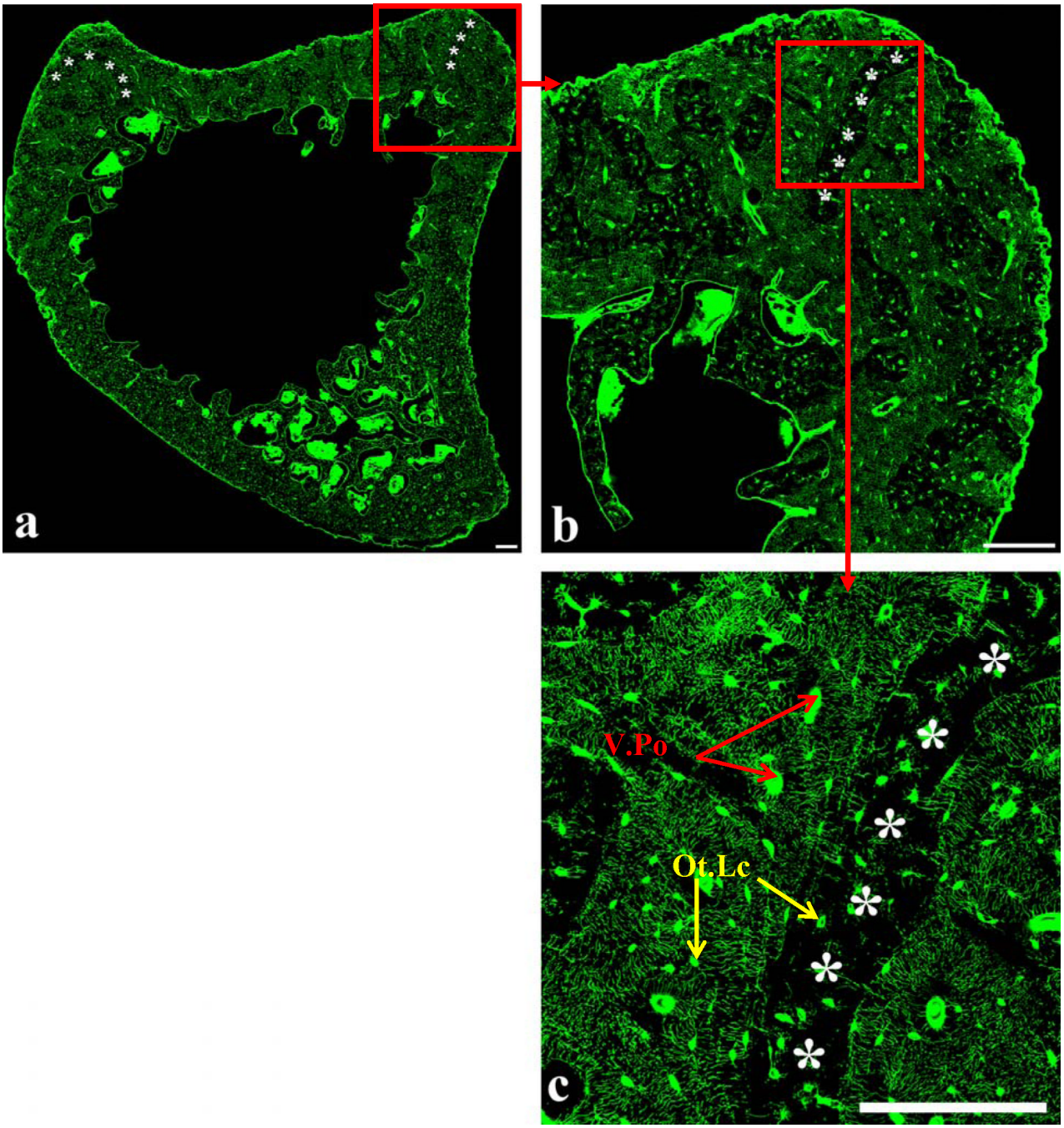

Figure 2.

(a) Reconstructed section from the metaphysis of the rat tibia, and enlargement of the areas delineated by the red squares (b, c). The reconstructed image enables visualization of bone macrostructure, the complexity of the lacunar-canalicular system, and areas with low canalicular density (asterisks). In (c) it is possible to clearly distinguish the inhomogeneous distribution of the lacunar-canalicular system, with areas of low canalicular density (asterisks) and areas of high canalicular density. Osteocyte lacunae (Ot.Lc) and vascular porosity (V.Po) are indicated in (c). Scale bars 60 μm.